EFFECT OF A DC ELECTRIC FIELD ON THE LIQUID-VAPOR INTERFACE IN A GROOVED FLAT HEAT PIPE

N. Cardin[1,2], M. Brik[1], S. Lips[1,*], S. Siedel[2], J. Bonjour[1] and L. Davoust[2]

[1]Univ Lyon, CNRS, INSA-Lyon, CETHIL UMR5008, F-69621, Villeurbanne, France

[2]Univ. Grenoble Alpes, CNRS, Grenoble INP, SIMaP, F-38000, Grenoble, France

*Author for correspondence

E-mail: stephane.lips@insa-lyon.fr

ABSTRACT

In this communication, a grooved flat plate heat pipe is considered with an electric field applied between the top and bottom plates of the heat pipe. In this way, a dielectric force arises, which aims at pumping the liquid phase together with the capillary force. The ability of the electric field to change the shape of the liquid-vapor interface is theoretically investigated by a numerical approach. This approach consists in the strong coupling between the Laplace-Young equation, extended with the electric stress, and the Poisson equation for the electric potential. The former is used for the calculation of the shape of the liquid-vapor interface while the latter is solved for the determination of the electric stress along the interface. The results show that the electric field can extend the capillary limit of the heat pipe by increasing the maximum curvature of the liquid-vapor interface before the meniscus recession. This effect is even greater than the electric pumping effect for non-wetting fluids. A final discussion is presented to highlight the configurations for which the use of an electric field yields significant improvements to the performance of a grooved flat plate heat pipe.

1   INTRODUCTION

Flat plate heat pipes are usually designed for thermal management of electronic components. They are passive devices made of a cavity filled by a two-phase working fluid. Like other heat pipes, they enable to transfer high heat fluxes with a low temperature gradient by means of the liquid-vapor phase change. However, these systems present various working limits which therefore lead to a limitation of the maximum heat flux that the system can transfer. The capillary limit is widely encountered in industrial applications. It occurs when the capillary structure cannot provide a high enough capillary pressure difference between the evaporator and the condenser to compensate for the pressure drops in the liquid and vapor phases. The use of an electric field to assist the capillary forces can enhance the heat pipe performance.

When two media are submitted to an electric field, an electric stress arises at the interface between the two media because of the jump of properties at the interface. Jones and Perry [1] and later Loehrke and Debs [2] showed that an electric field could be a

NOMENCLATURE

g	[m/s^2]	Gravity acceleration
h	[m]	Height
L_c	[m]	Capillary length
P	[Pa]	Pressure
q	[C/m^3]	Electric charge density
r	[m]	Radius of curvature
$\overline{\overline{T_e}}$	[N/m^2]	Electric stress tensor
$\vec{F_e}$	[N]	Volumic electric force
$\vec{E}$	[V/m]	Electric field
w	[m]	Width
x	[m]	Horizontal coordinate
z	[m]	Vertical coordinate
α	[-]	Apparent angle
ε	[F/m]	Permittivity
ε_r	[-]	Relative permittivity
θ	[-]	Contact angle
κ	[m^{-1}]	Interface curvature
ϕ	[-]	Angle between the tangent at the interface and the horizontal
ρ	[kg/m^3]	Density
σ	[N/m]	Surface tension

Subscripts

$edge$	Edge
f	Fins
g	Grooves
l	Liquid
n	Normal component
max	Maximal
t	Tangential component
v	Vapor

substitute for the capillary structure in heat pipes even though the performance was poor in comparison with the existing capillary driven heat pipe.

However, Bryan and Seyed-Yagoobi [3] managed to reach a 100% enhancement in the heat transport capability of a monogroove heat pipe with the use of DC electric fields at 20 kV. The fluid used in the experiment was R123.

Several numerical models available in the literature try to explain the EHD effect in a capillary groove. For instance, Suman [4] and more recently Saad et al. [5] developed a model taking into account both hydrodynamics and heat transfer in a capillary groove submitted to an electric field. But the theoretical approach of these models do not take into account the deformation of the liquid-vapoor interface due to the the electric stress. As a consequence, there is a need for a better understanding of the different mechanisms that govern the EHD effect in heat pipes.

The present communication is dedicated to the study of electric fields effects on the liquid-vapor interface shape in a rectangular groove. A model for local deformation of interfaces submitted to the EHD effect in a square groove is presented. It takes into account the gravitational and capillary forces, the pressure jump, as well as the electric stress at the liquid vapor interface.

2   GENERAL CONFIGURATION

The flat plate heat pipe geometry considered in this study is similar to that of Lips *et al.* [6]. It consists in a grooved copper plate and a transparent plate forming a sealed cavity, filled with FC-72 as working fluid (figure 1). The FC-72 is a dielectric fluid with an relative electric permittivity of 1.75 and it is used in electronic applications. This fluid is also used for actual experimental investigations.
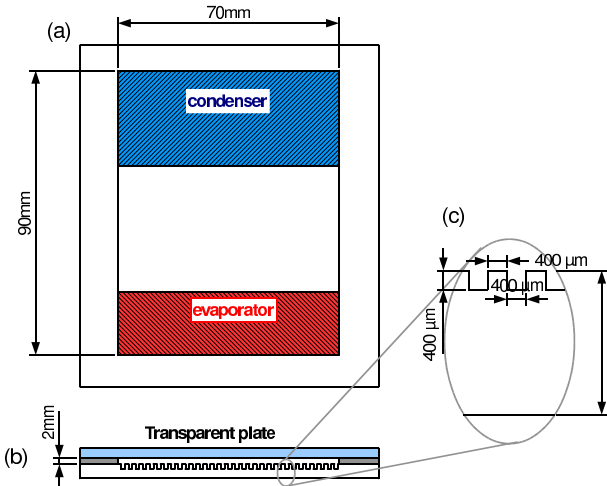

Figure 1.   Schematic of the flat plate heat pipe considered in the present study. (a) Top view, (b) lateral cross section and (c) close-up on the grooves cross section.

To study the effect of electric fields, the lower plate containing the grooves is used as the mass electrode. The upper plate is an assembly of different transparent layers to ensure experimental visualization. The upper part of the heat pipe is made of three different layers: a 5 mm thick polycarbonate plate, a thin 100 nm indium tin oxide (ITO) film glued on the polycarbonate plate with an optical glue and a 175 μm PET film to protect the ITO layer (figure 2). Table 1 lists the main geometric characteristics of the heat pipe.

w_f (μm)	h_g (μm)	w_g (μm)	h_v (μm)	h_{die} (μm)
400	400	400	1000	175

Table 1.   Geometry parameters

In a flat plate heat pipe, liquid and vapor flow are driven by the capillary pressure distribution along the heat pipe. The liquid evaporation at the evaporator side leads to higher meniscus curvatures than at the condenser side where condensation fills the grooves. This difference of curvature induces a gradient of pres-
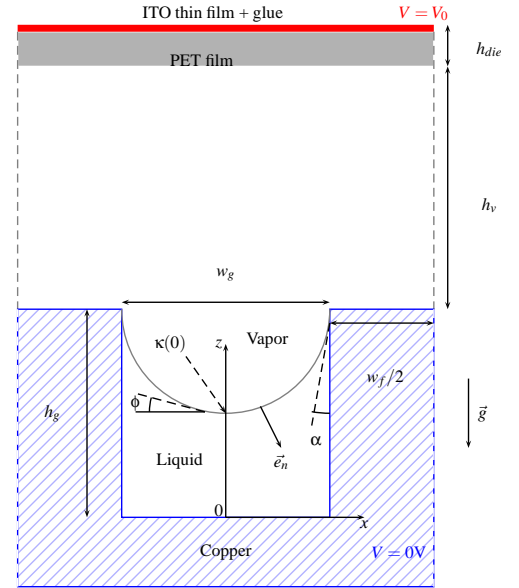

Figure 2.   Cross section of the electric flat plate heat pipe configuration

sure along the grooves which compensate for the pressure drops in the liquid and vapor phase (figure 3). Thus, the condensate is pumped back to the evaporator by the capillary flow. A number of limitations could affect the circulation of the working fluid for conventional flat plate heat pipe. When the pumping pressure produced by the grooves cannot overcome the sum of all pressure drops, the "capillary" limit is reached. This limitation is linked to the extremal curvature at the center of the interface in a groove. In practice, the value of the curvature is bounded by a maximal value corresponding to the recession of the meniscus inside the groove and a minimal value corresponding to the overflow of the liquid out of the groove. They both depend on the wettability of the fluid on the walls. Wettability is defined as the ability of a fluid phase to preferentially wet a solid surface in the presence of a second immiscible phase. The wettability can be represented by the contact angle θ. This angle is conventionally measured through the liquid, where a liquid-vapor interface meets a solid surface. The meniscus recession occurs at the evaporator when the dry out is reached leading to the maximal pressure jump at the liquid-vapor interface. At the meniscus recession, the apparent angle α equals the contact angle. The apparent angle is defined as the angle between the vertical wall and the tangent vector along the interface at the triple contact line. The maximal pressure jump at the center of the interface is expressed as follow:

$$\Delta P_{cap,max} = (P_v - P_l)_{max} = \sigma \kappa_{max} \qquad (1)$$

where σ the surface tension of the working fluid, κ_{max} the maximum curvature of the liquid-vapor interface and $\Delta P_{cap,max}$ the maximal pressure jump at the center of the interface.

In absence of electric field, the meniscus shape is governed by the capillary stress and the gravity. The capillary length is a characteristic length scale for an interface which is submitted both to
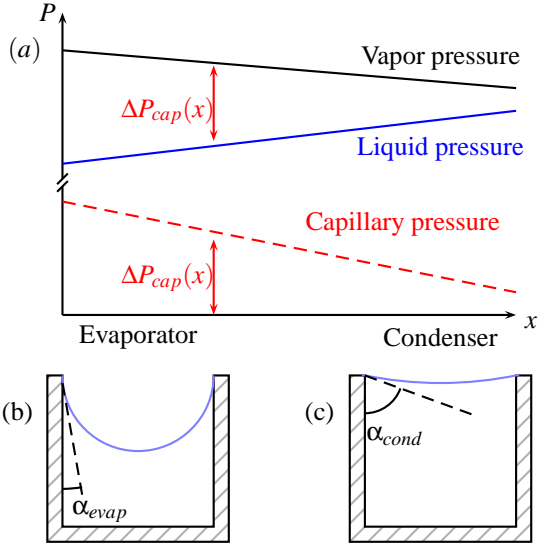
Figure 3. (a) Capillary pressure along a groove, (b) zoom on a cross section of a groove in the evaporator area and (c) zoom on a cross section of a groove on the condenser area

gravitational acceleration and to a surface force due to surface tension in the interface. The capillary length L_c is expressed as follows:

$$L_c = \sqrt{\left(\frac{\sigma}{\Delta\rho g}\right)} \tag{2}$$

where $\Delta\rho$ the liquid-vapor density difference and g the gravity acceleration. If the capillary length of the working fluid is much more greater than the width of the grooves, which is the case in the present study, then the shape of a cross section of the interface is mainly governed by the capillary stress and tend to be a portion of circle. The curvature κ of the interface depends on the difference of pressure between the vapor and the liquid phase. It can be positive, as presented in figure 3, or negative in the case of non wetting fluids. In the working geometry, the width of the groove is small enough to neglect the gravity force: the cross section of the meniscii are assumed to be a portion of circle. The maximal pressure jump at the center of the interface is expressed as follow:

$$\kappa_{max} = \frac{2\cos(\theta)}{w_g} \tag{3}$$

where w_g is the groove width.

When the liquid-vapor interface is submitted to an electric field, the resulting electric stress balances the capillary force. Because of the shape of the interface, the electric stress is not evenly distributed over the interface leading to local deformations. The resulting shape has no reason to be a portion of circle anymore.

3 MATHEMATICAL MODEL

The EHD phenomenon is governed by the forces acting on the surface between two fluids. The interfacial stress is linked to the jump of the Maxwell tensor at the interface. The Maxwell tensor

is expressed as [7]:

$$\overline{\overline{T_e}} = -\frac{1}{2}\varepsilon\left(\vec{E}.\vec{E}\right)\overline{\overline{I}} + \varepsilon\vec{E}\otimes\vec{E} \tag{4}$$

where $\overline{\overline{T_e}}$ is the Maxwell tensor. Considering the orthogonal system defined with the unit normal vector pointing from media 1 to media 2, the electric field can be defined as follow:

$$\vec{E} = \begin{bmatrix} E_n \\ E_t \end{bmatrix} \tag{5}$$

Based on the previous assumptions, the normal component of the electric stress is thus expressed by:

$$T_{e_n} = -\frac{\varepsilon_1}{2}\left(E_{n_1}^2 - E_{t_1}^2\right) + \frac{\varepsilon_2}{2}\left(E_{n_2}^2 - E_{t_2}^2\right) \tag{6}$$

Only the normal electric stress can deform the interface, whereas the tangential electric stress can create a flow in the phases. Here, only the normal electric stress is considered.

The meniscus shape in the absence of electric field is the result of the balance between the capillary force and the gravity. The Laplace-Young equation is used to link the curvature of the meniscus and the capillary pressure on the interface. In the presence of an electric field, the capillary stress and the electric stress are balanced with the pressure jump. Here, the curvature radius of the interface along the heat pipe axis is assumed to be infinite. For a meniscus, the extended Laplace-Young equation is verified all along the interface:

$$P_v - P_l = \kappa\sigma + T_{e_n} \tag{7}$$

where $P_l - P_v$ is the pressure difference between liquid and vapor phases, κ the local curvature. The electric field adds a normal stress on the meniscus T_{e_n}. The pressure difference between a point of the interface and the center of the interface is also due to the weight of the fluid. Thus:

$$\Delta\rho_l g z = P_l(z) - P_l(0) \tag{8}$$

where z is the height between the center of the meniscus and the given point at $z = 0$ Thus, the surface shape is determined by only one parameter, the pressure difference at the interface.

4 NUMERICAL PROCEDURE

The meniscus shape is numerically determined by an iterative methodology. The purpose of this methodology is to find the shape of the liquid-vapor interface at the equilibrium of the gravitational, capillary and electric forces. The software COMSOL Multiphysics is used to mesh the working geometry and to solve the distribution of the electric field. Matlab is used to determine the interface with an explicit scheme. The iterating numerical model evaluates the shape of the liquid-vapor interface for a given curvature at the center of the groove for various electric potential.

The electric field is firstly evaluated with COMSOL Multiphysics with an initial interface. Then the modified Laplace-Young equation is solved in Matlab and the new interface is export in Comsol. This procedure is iterated until convergence. This numerical methodology is faster than a moving mesh model

or a level set model.

4.1 Determination of the electric field

The working geometry consists of one rectangular groove. The groove is supposed to be infinite along the heat pipe axis and far enough from the edges of the heat pipe to neglect the effect of the side walls. The geometry is split in three different domains: the dielectric layer, corresponding to the PET film, the vapor phase and the liquid phase. Assuming that the media are linear, isotropic, homogeneous and with no charge density, the electric potential is found by solving the Poisson equation:

$$div\left(\sigma \vec{grad} V\right) = 0 \qquad (9)$$

An example of the field distribution evaluated in COMSOL is represented on figure 4. The field distribution is then exported in Matlab.
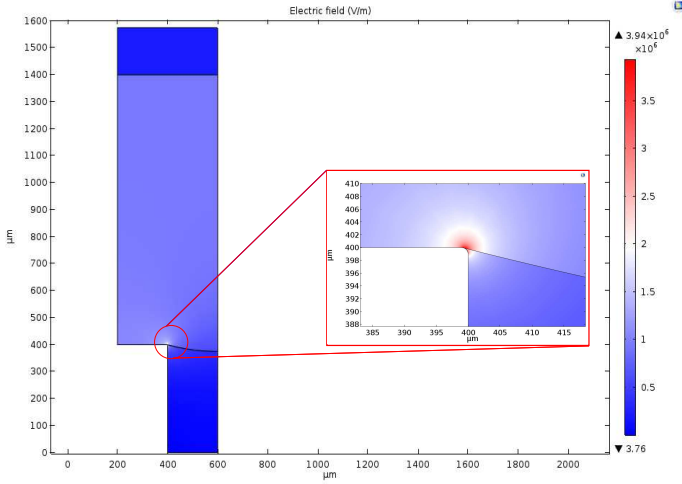

Figure 4. Exemple of the effect of electric field on the interface shape

4.2 Determination of the meniscus shape

The normal electric stress is evaluated in Matlab using the equation (6). From the value of the electric stress at each node on the interface, the new position of the nodes can be evaluated with the pressure difference between the node and the center of the interface.

$$P_l(z) - P_l(0) = \sigma\kappa(0) - \sigma\kappa(z) + T_{e_n}(0) - T_{e_n}(z) \qquad (10)$$

where $z = 0$ is taken at the center to the interface. A shooting method is used to verify the wettability condition on the edge. This method consists in an explicit scheme starting from the center of the interface:

$$\delta\phi = \frac{d\phi}{dx}\delta x = \frac{\kappa(0) + \frac{z(x)}{L_c^2} + \frac{T_{e_n}(0) - T_{e_n}(x)}{\sigma}}{\cos(\phi(x))}\delta x \qquad (11)$$

where ϕ is the angle between the tangent at the interface and $\vec{e_x}$ considering $z(0) = 0$ and $\phi(0) = 0$ to keep the symmetry. L_{cap} is the capillary length.

The new geometry is then exported as a spline curve in Comsol and a new mesh is built. The convergence was fund to be reached after 8 iterations.

4.3 Impact of the edge

In COMSOL, the edge of the fin is not represented by a sharp edge, but a circular arc to avoid divergence of the electric field in this area. The value of the edge radius is chosen to consider the rounded edge as a sharp edge from a mechanical point of view and to be greater than the minimum mesh element. A sensitivity study was conducted to determine the impact of the edge radius value. Figure 5 presents an example of the shapes of the interface close to the fin edges for various radii of curvature, with or without electric field. The curvature at the center of the interface is fixed with interface shape changes focused near the edges. Different values of r_{edge} are considered. These values are small enough to consider the edge as a sharp edge from a mechanical point of view. When no electric field is applied (solid lines), the three interfaces exhibit the same slope close to the triple contact line. The radius of curvature of the edge only affect the location of the triple contact line but has a low effect on the apparent angle. This is particularly true for values under $1\,\mu m$. In presence of an electric field (dashed lines), the apparent angle changes and becomes higher than in absence of electric field. The results show that all the three interfaces are almost the same in presence of an electric field for a given curvature at the center of the interface. The apparent angle and the pressure jump at the center
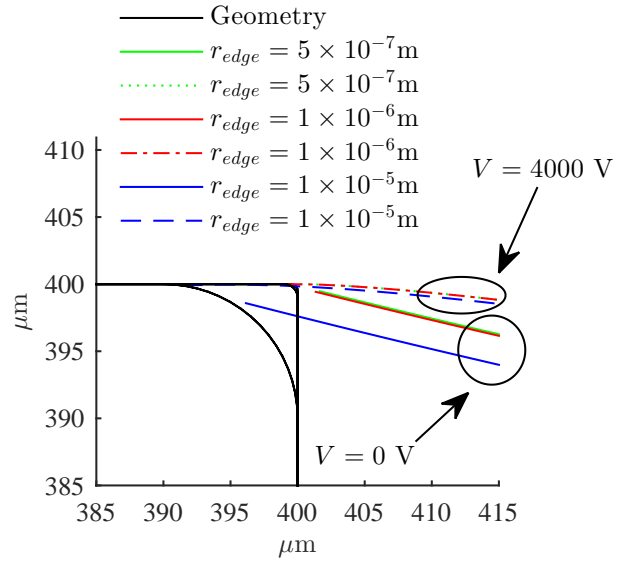

Figure 5. Effect of the edge radius on the meniscus shape.

of the interface in presence of an electric field in the same conditions as before are displayed on table 2. The results showed that the impact on the pressure jump is non significant (less than 0.1%).The impact on the apparent angle is also non significant (less than 1%). In presence of an electric field, the slope of the

liquid-vapor interface is not affected for small values of the edge radius, but the location of the triple contact is somewhat modified. Thus, in this study, r_{edge} is considered to be equal to $1\,\mu m$.

R_{edge} (m)	Pressure jump (Pa)	Apparent angle (°)
1×10^{-5}	22.563	91.9
5×10^{-6}	22.557	91.8
1×10^{-6}	22.552	91.6
5×10^{-7}	22.553	91.5

Table 2. Deformation of the interface for different radii

5 NUMERICAL RESULTS

5.1 Effects on the meniscus shape

In order to observe the impact of the electric field on the liquid circulation, the pressure jump at the liquid-vapor interface is plotted as a function of the curvature on figure 6. In the presence of an electric field, the pressure jump at the interface for a given curvature is larger than in the absence because of the sum of the electric and capillary forces. This effect is more important for low and negative curvatures than high and positive curvatures, which reduces the pumping effect on the fluid.
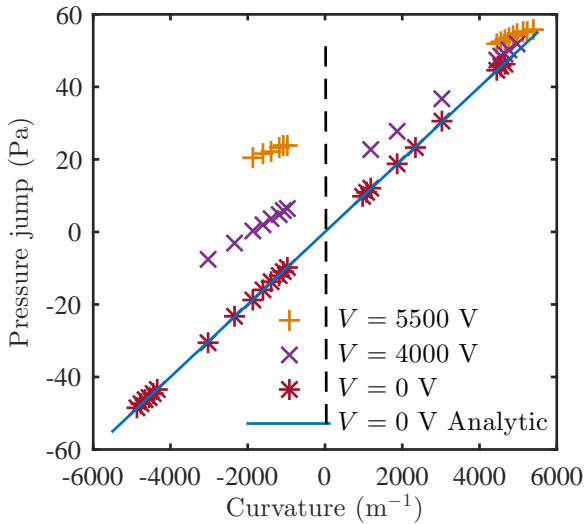

Figure 6. Effect on the pressure jump for FC-72.

An example of a deformed interface is given in figure 7. In this figure, only the sign of the curvature and the electric stress are modified. When the liquid-vapor interface is submitted to an electric field, the result is a high deformation of the liquid-vapor interface near the edge for a given curvature. The apparent angle is strongly modified by the electric field. The analytic solution for $V = 0\,V$ is deduced from equation (7)

The apparent angle is plotted as function of the curvature for different values of the electric potential on figure 8. For capillary
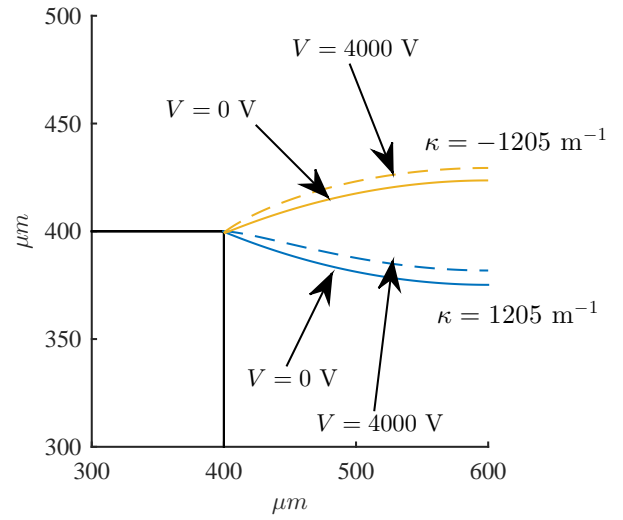

Figure 7. Exemple of the effect of electric field on the interface shape

force only the analytical solution is expressed as:

$$\alpha = acos(w_g * \kappa/2) \tag{12}$$

The numerical results for $V = 0\,V$ show a good correlation with the analytic solution, represented by the solid curve, meaning the meniscus is a portion of circle.
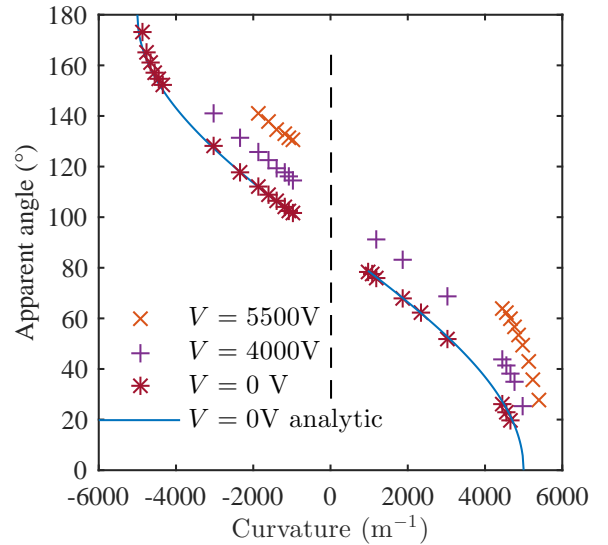

Figure 8. Effect of an electric field on the maximal pressure for FC-72.

For a given apparent angle, the presence of an electric stress leads to increased curvatures. The interface has no reason to be portion of circle. This effect is explained by the concentration of the electric field near the edges of the fin. The electric stress is pulling up the interface near the edge which results in higher curvature in the center of the meniscus. For the same apparent angle, the higher the electric potential, the greater the deforma-
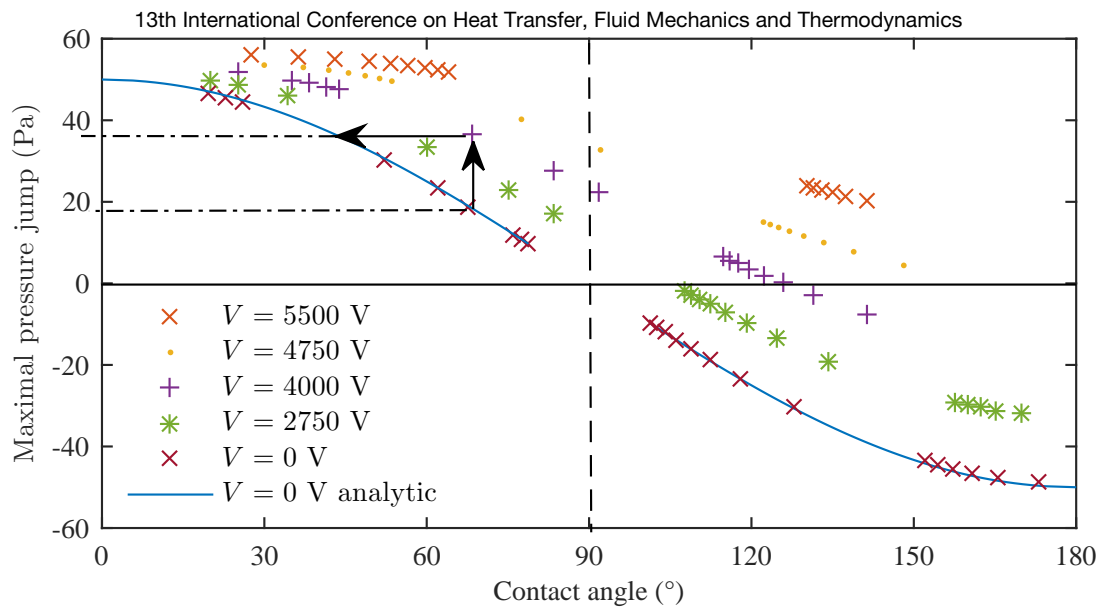
Figure 9. Effect of an electric field at meniscus recession for FC-72.

tion. This effect could be used at the evaporator to increase the heat flux corresponding to the capillary limit.

5.2 Effects on the heat pipe performance

At the meniscus recession, the contact angle and the apparent angle become equal and the pressure jump at the interface is found maximum. Figure 9 shows the maximal pressure jump as function of the contact angle. The analytical solution is deduced from equation (7) and equation (12) with $\alpha = \theta$.

The results highlights greater maximal pressure jump at the interface in the presence of electric stress. If the effect of electric field is only concentrated over the evaporator area, possible enhancement of the capillary limit could be obtained. In the presence of an electric stress ($V = 4000\,\text{V}$), the maximal pressure jump on the interface doubles for a contact angle of $70\,^\circ$ ($19\,\text{Pa}$ for $V = 0\,\text{V}$ compared to $38\,\text{Pa}$ in the presence of electric stress). This effect is even greater for non wetting fluids for which the sign of the maximal pressure jump can be reversed.

6 CONCLUSION

A theoretical model was developed to analyze the deformation of a meniscus in a flat plate heat pipe submitted to EHD effects. The model is based on the modified Laplace-Young equation and the Poisson equation. The Laplace-Young equation is modified in order to take into account the electric stress. The model is able to predict the shape of a meniscus for a given electric field. The results show a high concentration of the electric stress near the edges, which pulls up the interface and which yields higher curvatures. This suggests that, contrary to the current state-of-the-art on heat pipes, non wetting fluids might be used as working fluids. The capillary limit can be extended in presence of an applied electric field. Capillary pressure is reduced when the

electric field is applied all along the grooves. In order to enhance the performance of the heat pipe, the electrode should be placed over the evaporator area.

Further experimental investigations on the shape of an interface submitted to an electric field are expected for both isothermal and non-isothermal conditions.

REFERENCES

[1] Jones T. B. and Perry M. P., Electrohydrodynamic heat pipe experiments, *Journal of Applied Physics*, vol. 45, No. 5, pp. 2129-2132, May 1974.

[2] Loehrke R. and Debs R., Measurements of the performance of an electrohydrodynamic heat pipe, *In 10th Thermophysics Conference*, Denver, Colorado, vol. 68, pp. 197-200, 27-29 May 1975.

[3] Bryan J. E., Seyed-Yagoobi J., Heat transport enhancement of monogroove heat pipe with electrohydrodynamic pumping, *Journal of Thermophysics and Heat Transfer*, vol 11, No. 3, pp. 454-460, 1997.

[4] Suman, B., A steady state model and maximum heat transport capacity of an electrohydrodynamically augmented micro-grooved heat pipe, *International Journal of Heat and Mass Transfer*, vol 49, No. 21-22, pp. 3957-3967, 2006.

[5] Saad I., Maalej S., Zaghdoudi M. C, Modeling of the EHD effects on hydrodynamics and heat transfer within a fl at miniature heat pipe including axial capillary grooves, *Journal of Electrostatics*, vol 85, pp. 61-78, 2017.

[6] Lips S., Lefèvre F., Bonjour J., Physical mechanisms involved in grooved flat heat pipes: Experimental and numerical analyses, *International Journal of Thermal Sciences*, vol 50, No. 7, pp. 1243-1252, 2011.

[7] Melcher J. R. and Taylor G. I., Electrohydrodynamics: A Review of the Role of Interfacial Shear Stresses, *Annual Review of Fluid Mechanics*, vol 1, No. 1, pp. 111146, 1969.